SUPPORTING INFORMATION

TABLE OF CONTENTS

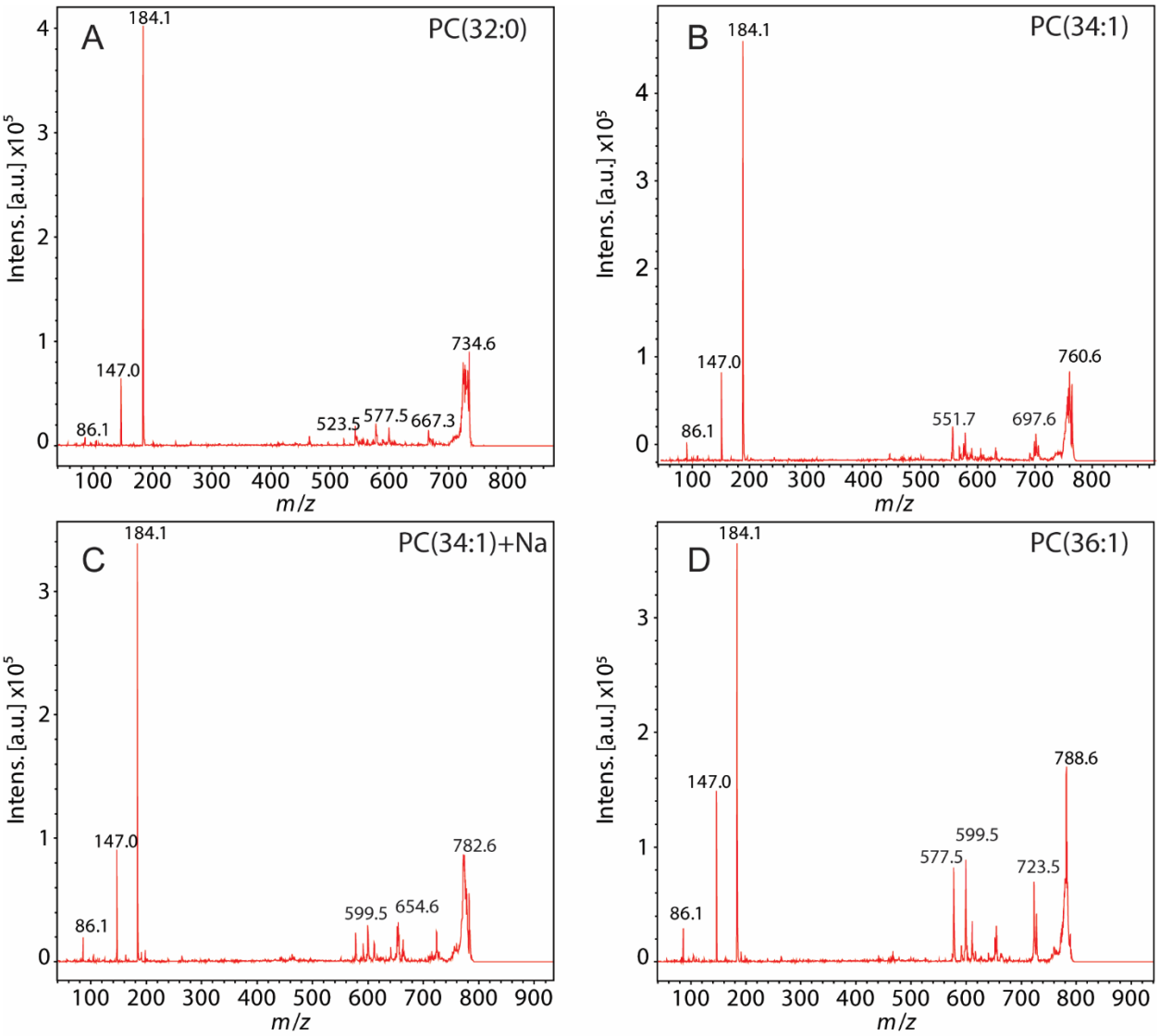

Figure S1. Tandem mass spectra of major lipids. (A) PC(32:0) at *m/z* 734.6, (B) PC(34:1) at *m/z* 760.6, (C) PC(34:1)+Na at *m/z* 782.6 and (D) PC(36:1) at *m/z* 788.6. Important fragments include *m/z* 184.1 (PC head group, $C_5H_{15}NPO_4$), *m/z* 147 (sodiated PC head group without trimethylamine, $C_2H_5PO_4Na$). Higher mass fragments are associated with the loss of PC headgroup or trimethylamine.

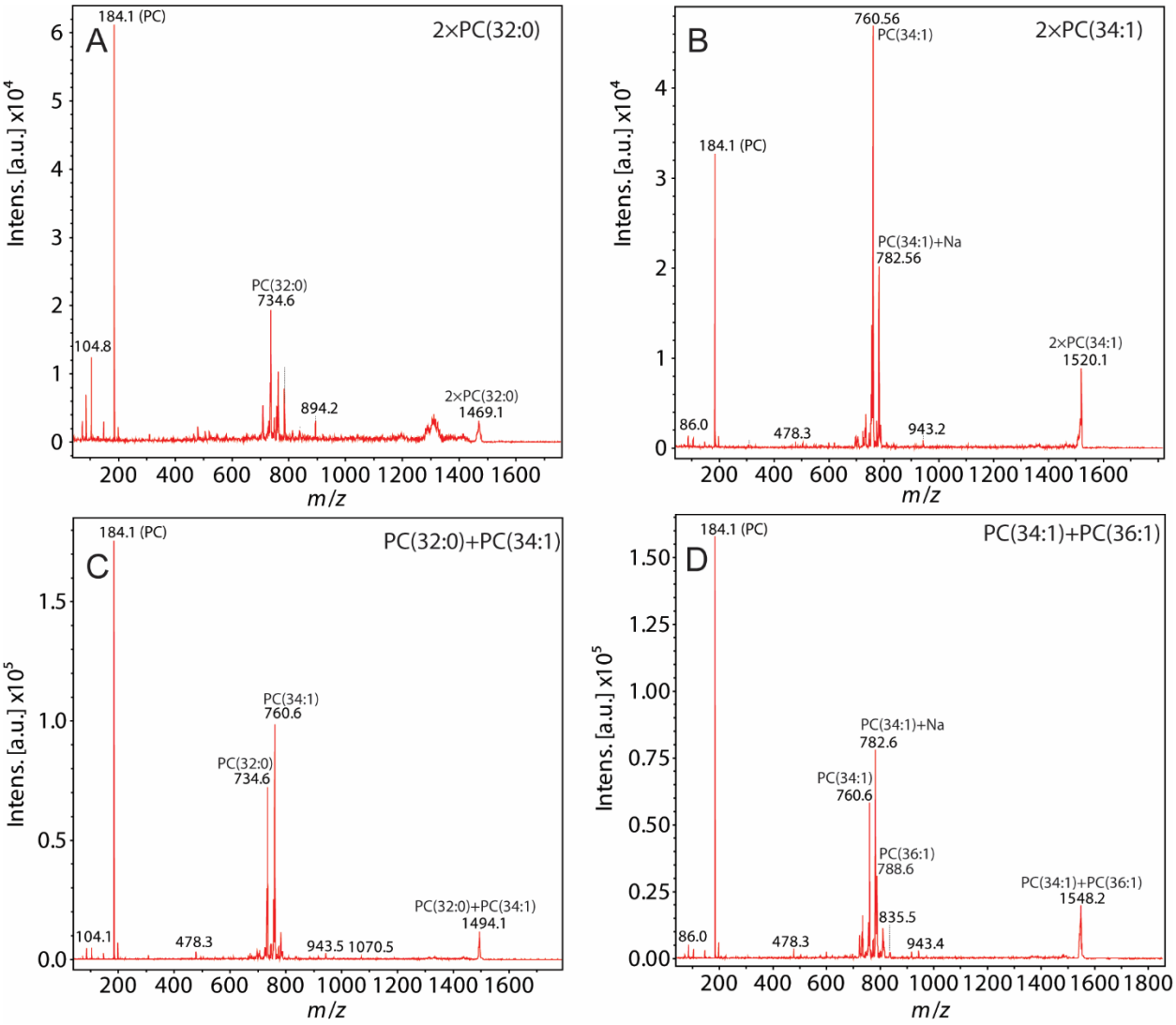

Figure S2. Tandem mass spectra of lipid dimers. (A) Homodimer of PC(32:0) at *m/z* 1469.1, (B) homodimer of PC(34:1) at *m/z* 1520.1, (C) hetero-dimer of PC(32:0) and PC(34:1) at *m/z* 1494.1 *m/z*, and (D) hetero-dimer of PC(34:1) and PC(36:1) at *m/z* 1548.2.

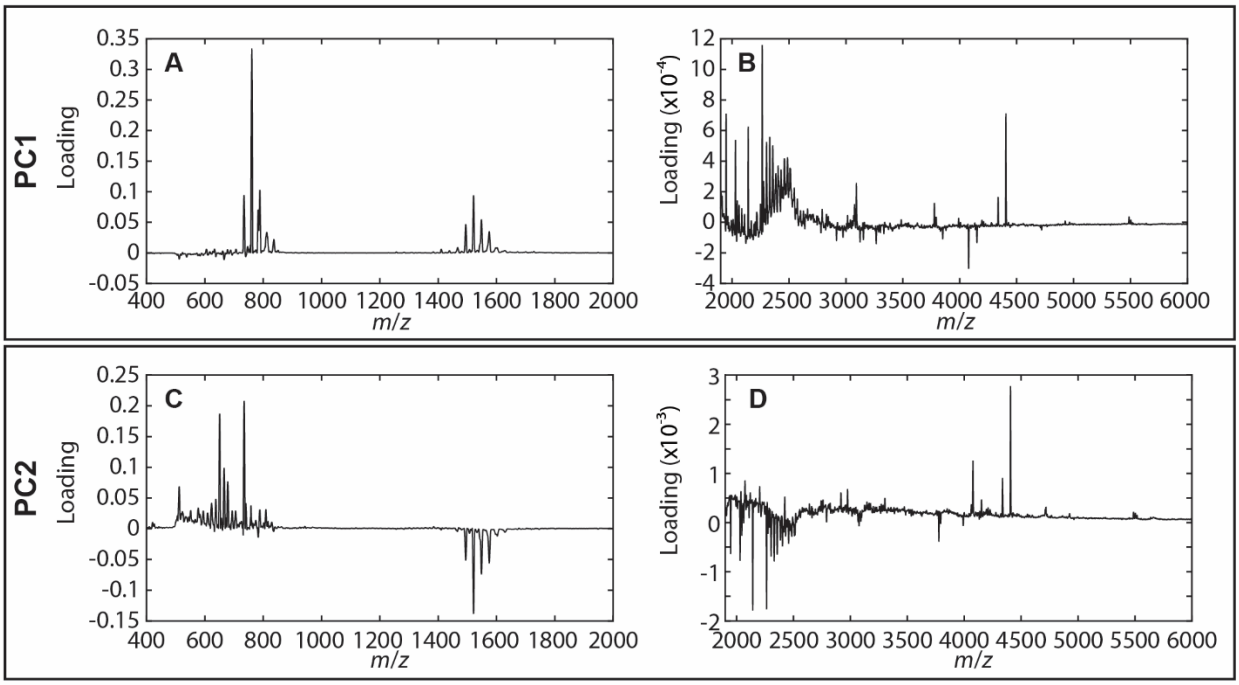

Figure S3. Principal component (PC) 1 and 2 obtained from PCA of LM single cell mass spectra. Note that comparing the two PCs in the mass range of *m/z* 1,900–6,000, the loading score of PC2 is higher than PC1 (10^{-3} vs. 10^{-4}), suggesting that variation in PC2 is more sensitive to heterogeneity in the putative peptides.

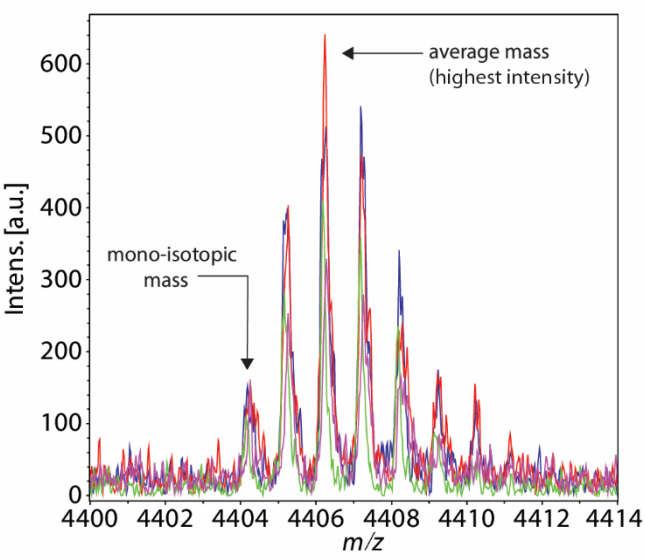

Figure S4. The isotopic pattern of the TOF mass spectral peak with highest intensity at *m/z* 4406. The data were rendered from mass spectra of four cells.

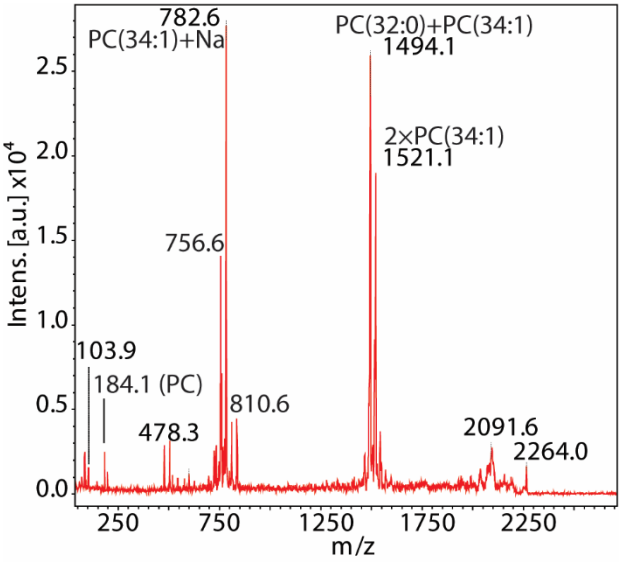

Figure S5. The product-ion mass spectrum of *m/z* 2263 (±5 Da precursor mass selection window) obtained by random continuous acquisition of data from many cells; cell clusters yielded intense peaks corresponding to lipids.

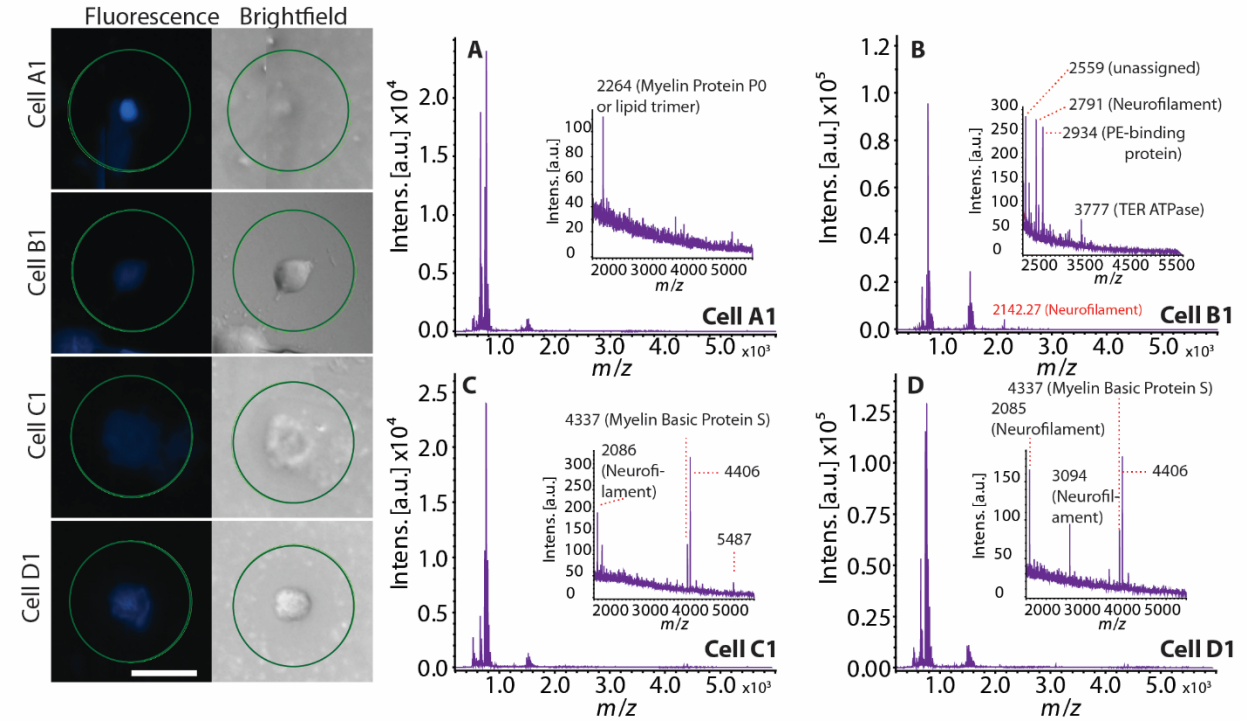

Figure S6. Representative mass spectra of individual DRG cells. The optical images of the cells are shown in the left panels. The scale bar is 50 μm. These cells have similar mass spectra to the cells A–D shown in Figure 4 of the main text (e.g., cell A1 is similar to cell A, cell C1 similar to cell C, and D1 to D). However, the cells were from different animals and sample slides, and analyzed in a different batch as compared to the cells in Figure 4.

(A) Cell A1 is a small cell with an intense nuclear stain. The mass spectrum shows good lipid signals but no additional peaks except *m/z* 2264. (B) Cell B1 shows a signal of *m/z* 3777 in addition to other peptides, including putative lipid binding protein. (C) Cell C1 is a large, perhaps damaged cell. (D) Cell D1 is an intact large cell. Note that cells C1 and D1 are 8.5 mm apart on the sample slide, suggesting that the detection of similar compounds, such as *m/z* 4406, is not based on cell location on the slide.

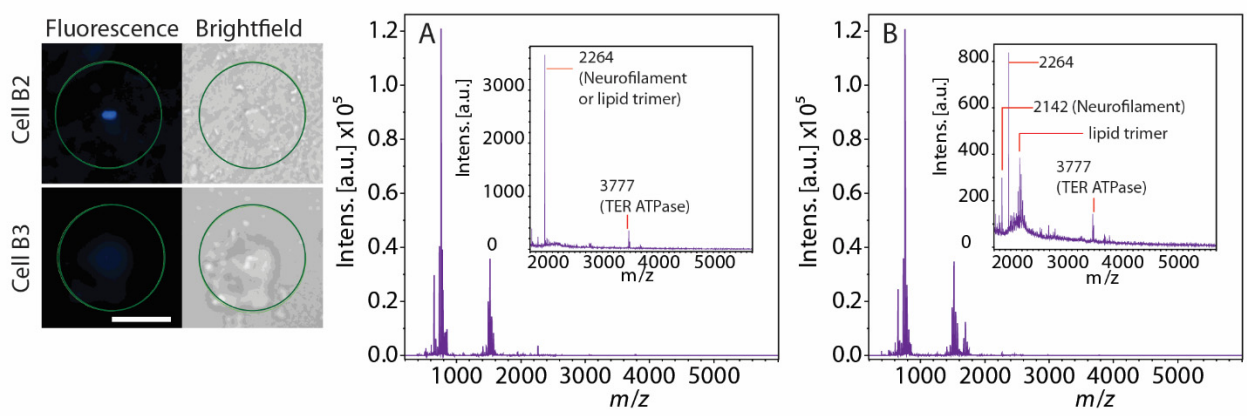

Figure S7. Representative LM mass spectra of individual DRG cells. The optical images of the cells are shown in the left panels. The scale bar is 50 μm. (A, B) Mass spectra of cells B2 and B3 obtained from LM analysis, respectively. These cells contain *m/z* 3777, which is tentatively assigned to a nuclear peptide (TER ATPase). Because cell B, shown in Figure 4B of the main text and as cell B1 in panel B, Figure S6, also contain *m/z* 3777, we refer to these two cells here as cells B2 and B3.

Cells B2 and B3 are 5.5 mm apart on the sample slide. Note that mass spectral type B is defined by the presence of *m/z* 2142. Cell B3 shows the presence of *m/z* 3777, and thus belongs to type B. This suggests that *m/z* 3777 cannot be used to define a third mass spectral cell type.

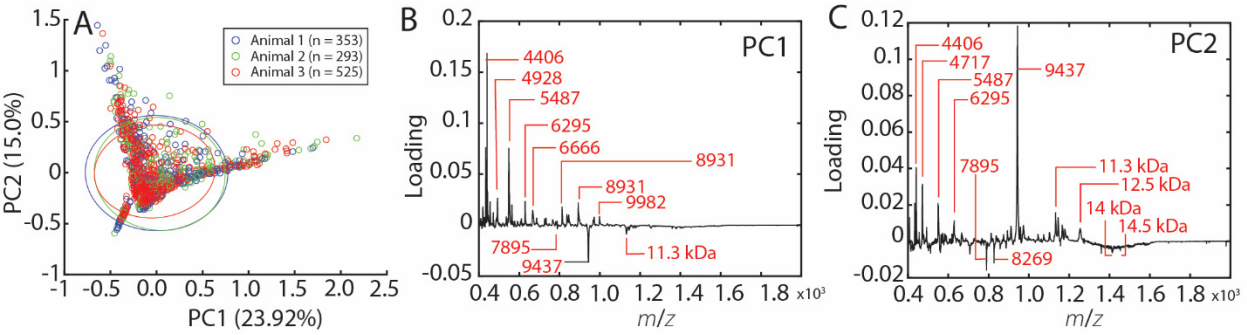

Figure S8. (A) PCA of HM data demonstrating substantial overlap of data acquired from cells collected from three animals. (B) PC1 and (C) PC2. From PC2, *m/z*s containing the largest positive and negative loadings were selected for a targeted comparative analysis.

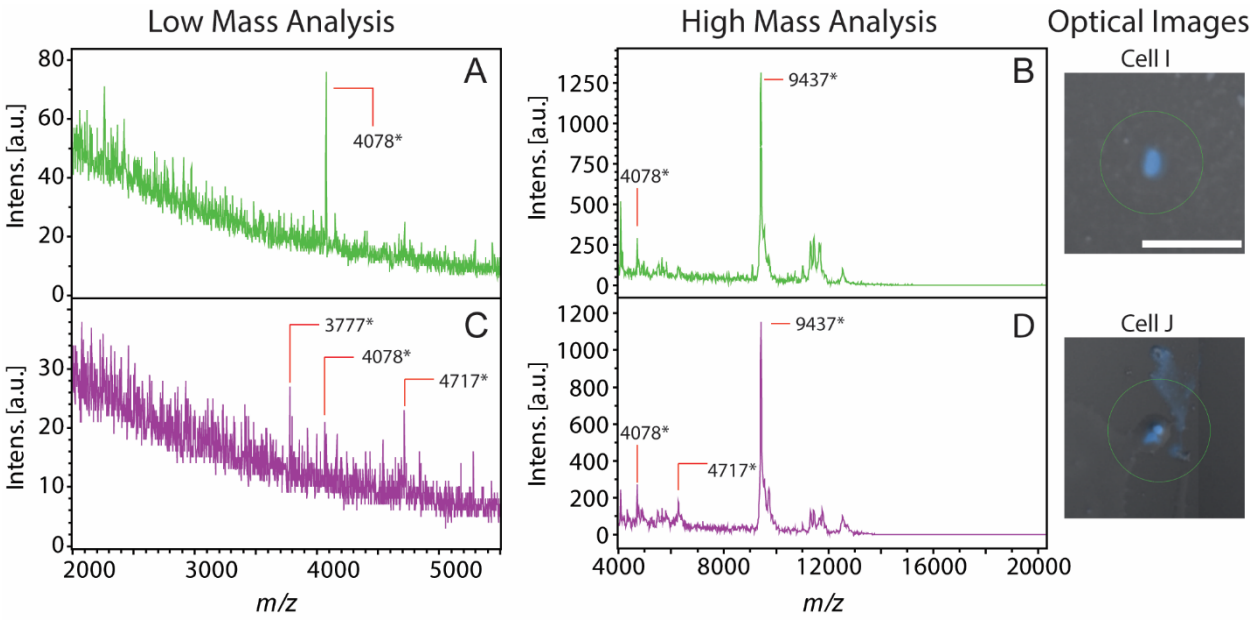

Figure S9. Representative (A, C) LM and (B, D) HM raw mass spectra and optical images of two type C cells. The scale bar is 100 μm. The asterisks note that the *m/z* values are not monoisotopic.

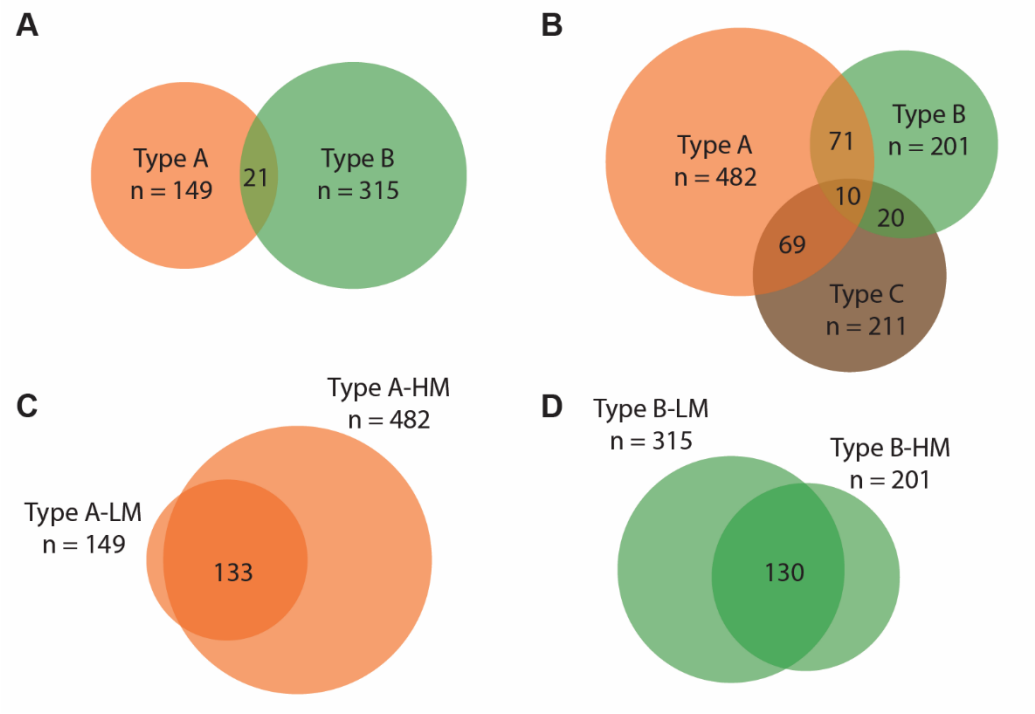

Figure S10. Population overlap for observed cell types. Overlap between (A) A-type and B-type peptide markers for LM peptide markers **only**, (B) A-type, B-type, and C-type peptide markers for HM peptide markers **only**, (C) LM and HM A-type peptide markers, and (D) LM and HM B-type peptide markers. *Note: since there are no peptide markers for LM-C, we did not show the overlap between type C-LM with other subpopulations.*

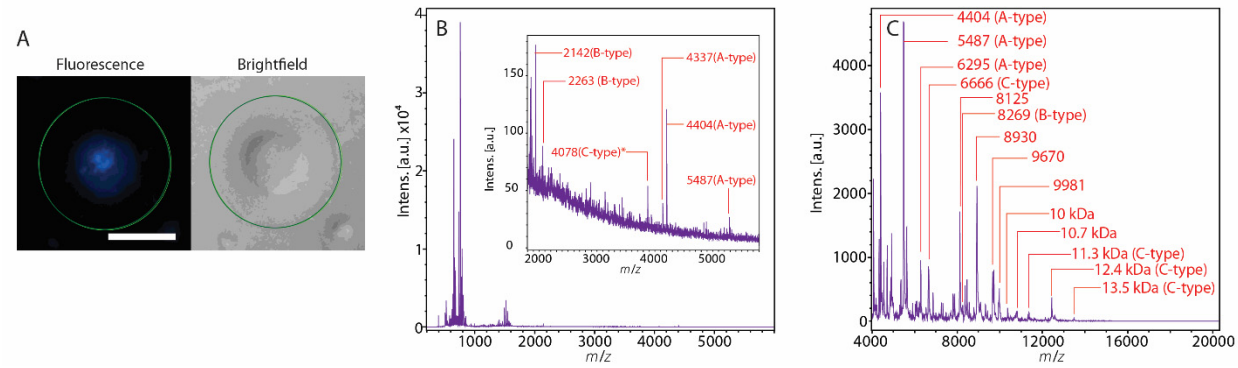

Figure S11. (A) Optical images and (B) LM and (C) HM mass spectra of a single DRG cell shared among A, B and C-type.

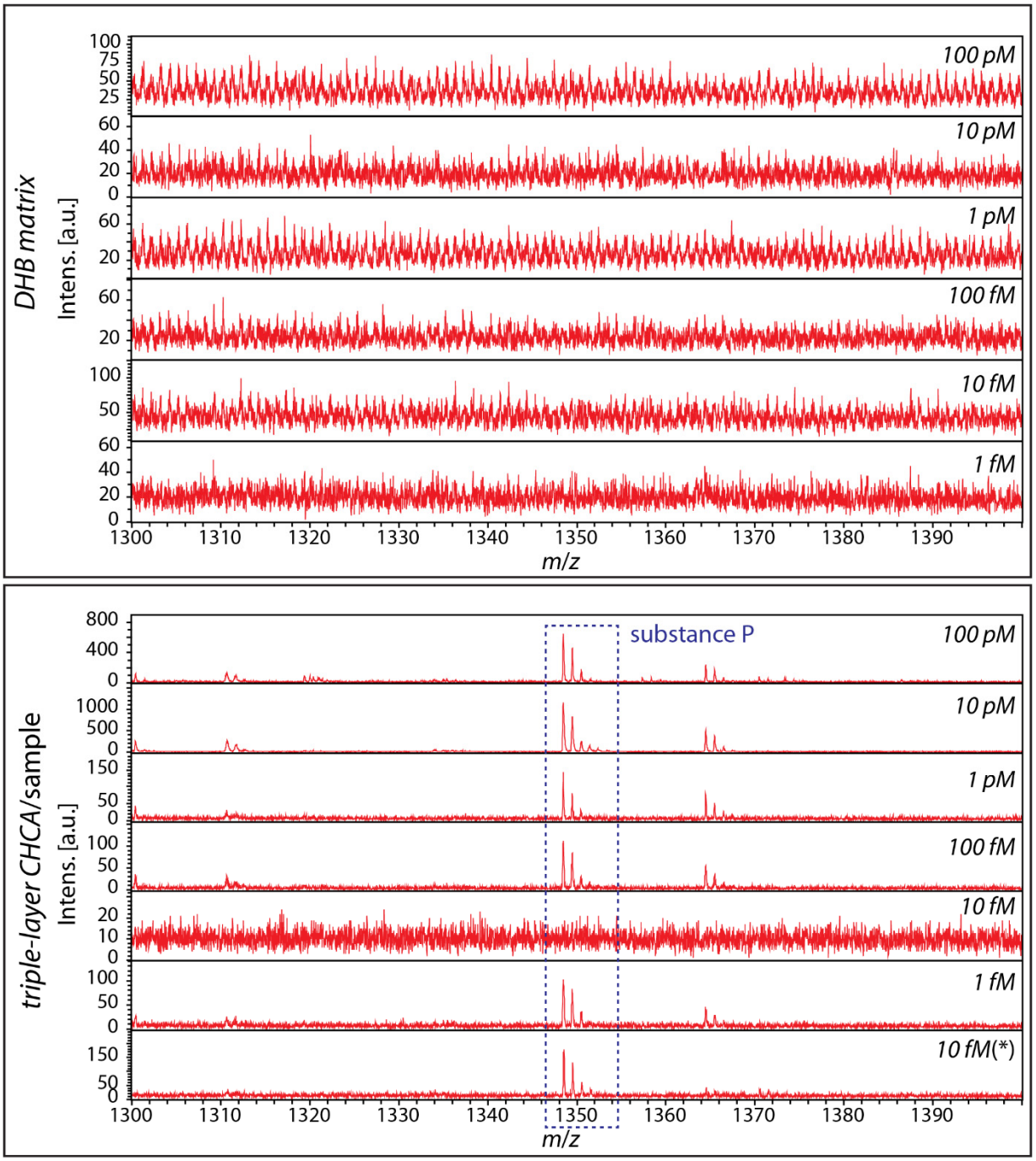

Figure S12. The detectability of a substance P standard at various concentrations from 100 pM to 1 fM using a traditional DHB matrix application (top) versus a triple-layer CHCA/sample application (bottom). Each data set was collected on the same day and on the same substrate, unless indicated with the asterisk. One panel at 10 fM for the triple-layer application did not show the signal of substance P, which is likely due to irregularities in the crystal layer. Therefore, another mass spectrum at the same concentration collected on a different day is shown (10 fM(*)). Each spectrum was generated after 300 laser shots. For DHB, the laser power was about twice that used for CHCA (65 versus 35 arbitrary units).

Table S1. List of observed *m/z* values from MALDI-TOF MS single cell profiling experiments and mass-matched corresponding peptides detected in previous LC-MS peptidomics study (reference 35 in the main text). In the case where there is more than one potential match, the bolded entries indicate the peptide fragment that was more likely to be detected because other fragments of the same protein were also detected. Some peptides of myelin proteins and neurofilaments were observed in morphologically specific sensory-motor system regions (i.e., ventral root, dorsal root, etc.) in the previous LC-MS study.

Observed m/z	***Protein Name***	***Peptide Fragment***	***Theoretical m/z***
1947	**Myelin Protein P0**	**K.AASEKKSKGLGESRKDKK**	1947.09
	Histone H4	I.RDAVTYTEHAKRKTVTA.M	1947.03
2031	**Vimentin**	**L.LIKTVETRDGQVINETSQ.H**	2031.06
	Adducin 3 isoform CRA_b	F.RTPSFLKKNKKKEKVEA	2031.20
	Histone H2A type 1C	L.AGNAARDNKKTRIIPRHL.Q	2031.16
2086	**Neurofilament medium polypeptide**	**P.SAYRRVPTETRSSFSRVS.G**	2086.07
	Hemoglobin alpha adult chain 2	H.ASLDKFLASVSTVLTSKYR	2086.15
2141	**Neurofilament heavy polypeptide**	**D.Q(-17.03)KDSQPSEKAPEDKAAKGDK**	2140.99
	Fibrinogen beta chain	L.V(+42.01)QTQAAT(+79.97)TDSDKVDLSIAR.G	2141.00
2263	**Myelin Protein P0**	**R.STKAASEKKSKGLGESRKDKK**	2263.27
2792	Neurofilament light polypeptide	M.S(+42.01)SFSYEPYFSTSYKRRYVETPR.V	2792.32
2920	**Neurofilament medium polypeptide**	**S.GSPSSGFRSQSWSRGSPSTVSSSYKRSA.L**	2920.39
	Tubulin beta-5 chain	W.AKGHYTEGAELVDSVLDVVRKEAESCD.C	2920.39
2934	Phosphatidylethanolamine-binding protein 1	M.KGNDISSGTVLSEYVGSGPPKDTGLHRY.V	2934.45
2976	Protein LOC680353	TLVITDKEKAEKLKQSLPPGLAVKELK	2976.76
	Galectin-1	A.DLTIKLPDGHEFKFPNRLNMEAINY.M	2975.50
3015	**Neurofilament medium polypeptide**	**D.VSPAEEKKGEDRSDDKVVVTKKVEKIT.S**	3014.63
	Catenin beta-1	M.A(+42.01)TQADLMELDMAMEPDRKAAVSHWQQ.Q	3014.37
	Protein RGD1308134	VSDSSPAGAQIKTTVKRKVYEDSGIPLPA	3014.63

3074	**Myelin Protein P0**	**Y.AMLDHSRSTKAASEKKSKGLGESRKDKK**	3073.65
	Neurofilament medium polypeptide	**T.VTQKVEEHEETFEEKLVSTKKVEKVT.S**	3074.62
3093	**Neurofilament medium polypeptide**	**K.VEAPKLKVQHKFVEEIIEETKVEDEK(-.98).S**	3093.68
		K.VEAPKLKVQHKFVEEIIEETKVEDEK.S	3094.66
3304	Heat shock protein beta-1	PFSLLRSPSWEPFRDWYPAHSRLFDQA	3305.62
	40S ribosomal protein S12	M.A(+42.01)EEGIAAGGVMDVNTALQEVLKTALIHDGLAR.G	3304.71
3777	Transitional endoplasmic reticulum ATPase	A.RGGNIGDGGGAADRVINQILTEMDGMSTKKNVFIIGA.T	3775.91
3989	**Myelin Protein P0**	**R.GRQTPVLYAMLDHSRSTKAASEKKSKGLGESRKDKK**	3988.14
4078	--	--	--
4151	--	--	--
4337	**Myelin basic protein S**	**KNIVTPRTPPPSQGKGRGLSLSRFSWGGRDSRSGSPMARR**	4337.3
4406	--	--	--
4717	**Thymosin beta-4**	**D.KPDMAEIEKFDKSKLKKTETQEKNPLPSKETIEQEKQAGES**	4717.42
4926	--	--	--
4963	**Thymosin beta-4**	**M.S(+42.01)DKPDMAEIEKFDKSKLKKTETQEKNPLPSKETIEQEKQAGES**	4961.49
5487	--	--	--